THE JOURNAL OF PHYSICAL CHEMISTRY B

Article

pubs.acs.org/JPCB

Electronic Excitations in Nonpolar Solvents: Can the Polarizable Continuum Model Accurately Reproduce Solvent Effects?

Lorenzo Cupellini,* Claudio Amovilli,* and Benedetta Mennucci*

Dipartimento di Chimica e Chimica Industriale, University of Pisa, Via Risorgimento 35, 56126 Pisa, Italy

Supporting Information

ABSTRACT: In nonpolar solvents, both electrostatic and nonelectrostatic interactions play a role in tuning the electronic excitations of molecular solutes. This specificity makes the application of continuum solvation models a challenge. Here, we propose a strategy for the calculation of solvatochromic shifts on absorption spectra, using a coupling of the polarizable continuum model with a time-dependent density functional theory framework, which explicitly accounts for dispersion and repulsion, as well as for electrostatic effects. Our analysis makes a step further in the interpretation of the effects of nonpolar solvents and suggests new directions in their modeling using continuum formulations.

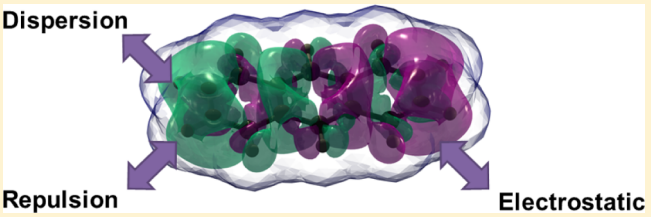

1. INTRODUCTION

Environmental effects play a crucial role in tuning the optical properties of molecules and the corresponding electronic spectroscopies. In quantum chemistry, these effects are commonly dealt with by introducing an interaction term in the molecular Hamiltonian, as in the so-called *effective Hamiltonian* methods. These methods include both the quantum mechanics/molecular mechanics (QM/MM) models, which adopt a classical but atomistic description of the environment,[1−6] and the QM/continuum models, which describe implicitly the environment as a structureless dielectric medium.[7−11] Both QM/MM and QM/continuum models have in common the classical electrostatic nature of the QM/classical interaction potential. On the contrary, nonelectrostatic interactions (namely dispersion and repulsion) are usually associated with classical potentials, disregarding their quantum-mechanical origin; dispersion is indeed a nonlocal electron correlation effect, whereas repulsion arises from the Pauli exclusion principle. Attempts to describe dispersion and repulsion effects through quantum-mechanical approaches have already been proposed within QM/continuum models. The self-consistent model of Amovilli and Mennucci[12] developed reformulating the theory of weakly interacting systems within the polarizable continuum model (PCM)[11] is an example of such attempts, together with the model recently developed by Pomogaeva and Chipman from a density functional formulation of dispersion energy.[13,14]

In the large majority of cases, however, both QM/MM and QM/continuum models have been employed in the treatment of solvent effects on electronic spectroscopies such as absorption, fluorescence, and circular dichroism by limiting the solute−solvent interactions to the electrostatic one.[5,15,16] On the contrary, nonelectrostatic interactions, and particularly dispersion, are expected to significantly affect the electronic spectra in solution, especially when the solvent is nonpolar. In 1950, Bayliss proposed the first continuum model to explain the dispersion shift in nonpolar solvents, which was related to the oscillator strength of the transition and to the square of the refractive index.[17] Another approach was proposed by Rösch and Zerner within a QM description by calculating dispersion effects on the excitation energies as difference in the dispersion stabilization energy from ground to excited state obtained at a semiempirical configuration interaction (CIS) treatment of both solute and solvent molecules.[18] In more recent years, the interest in the modeling of dispersion effects on solvatochromic shifts has grown further, and several steps ahead have been made. A semiclassical expression has been derived by Renger et al.,[19] under a dipole approximation. The model by Amovilli and Mennucci[12] has been extended to electronic excitations by Weijo et al.[20] More recently, Marenich et al.[21] proposed a state-specific polarizability model (SMSSP) for dispersion and applied that to the calculation of solvatochromic shifts of aromatic hydrocarbons in nonpolar solvents. The SMSSP model was successively coupled to a state-specific description of the electrostatic effects to calculate solvatochromic shifts of polar chromophores in water and methanol.[22]

All these developments have led us to reconsider the problem of the applicability of continuum models to describe solvent effects in the excitations of molecular solutes in nonpolar solvents. In particular, we focus here on the PCM formulation of continuum models and we investigate the contribution that each interaction (electrostatic, repulsive, and dispersive) has on the excitation energies of valence transitions of a selected set of polar and apolar solutes in a nonpolar solvent and the possible couplings among them. This analysis is

Special Issue: Branka M. Ladanyi Festschrift

Received: August 6, 2014
Revised: September 25, 2014

dx.doi.org/10.1021/jp507962n | J. Phys. Chem. B XXXX, XXX, XXX−XXX

performed by applying the time-dependent formulation of density functional theory (DFT) and the role played by the chosen functional is evaluated together with the impact that different formulations of the electrostatic contribution have on the accuracy of the correlation with experimental solvatochromic shifts.

The paper is organized as follows. In section 2, we present the methodological aspects related to the calculation of solvent effects in electronic excitations with the PCM, in section 3 we report the computational details, and in section 4, we present a detailed analysis of the results. We conclude with a brief summary in section 5.

2. METHODS

In short, the PCM description of the electrostatic solute−solvent interaction including polarization effects is through the introduction of an apparent surface charge (ASC) density σ supported on the surface Γ of the cavity which contains the QM solute:

$$W_{ele} = \int_{\Gamma} ds\ \sigma[\varepsilon,\rho](s)\ V[\rho](s) \tag{1}$$

where $V[\rho]$ is the electrostatic potential generated by the QM solute (here represented in terms of its charge distribution ρ) and ε is the solvent dielectric constant. σ is obtained as the solution of a specific integral equation: various alternative expressions of this equation have been given during the years leading to different formulations of the PCM, known as D-PCM,[23,24] C-PCM,[25] and IEF-PCM.[26] In all cases, the surface charge will depend on the shape of the cavity and on the electrostatic potential (or field) generated by the QM solute on the surface. Commonly, a numerical representation of σ is used introducing a mesh of the cavity surface and replacing the continuous ASC distribution with point like charges.

Moving to Pauli repulsion and dispersion interactions, Amovilli and Mennucci's approach[12] is here adopted. In short, the Pauli repulsion contribution is derived from the exchange and penetration terms of the decomposition of the intermolecular interaction energy. A simplified expression for a uniform solvent, which takes into account its continuum nature is then obtained:

$$W_{rep} = k_{rep}\frac{\rho_S n_S^v}{M_S}\int_{r\notin C} dr\ \rho(r) \tag{2}$$

where k_{rep} is a suitable scaling parameter, ρ_S is the density of the solvent relative to water at 298 K, n_S^v is the number of valence electrons in the solvent molecules, and M_S is their molecular weight. Equation 2 shows that the repulsion interaction is proportional to the so-called "escaped charge": the electronic density which extends beyond the boundaries of the molecular cavity.

The expression for the dispersion energy is instead achieved by similarity with electrostatics introducing another ASC density induced on the cavity surface by the transition charge density ρ_p and depending on a dielectric constant calculated at imaginary frequencies, $\varepsilon(i\omega)$. By assuming $\sigma[\varepsilon(i\omega),\rho_p]$[27] to be proportional to the corresponding electrostatic field generated by ρ_p, one can write the interaction energy as[12]

$$W_{disp} = -k_{disp}\frac{\eta_S^2 - 1}{\eta_S^2}\sum_p \frac{\Omega^S}{\Omega^S + \omega_p}\int_{\Gamma} ds\ V_p(s)\ E_p(s) \tag{3}$$

where the index "p" runs over the excited states of the solute, ω_p is the corresponding excitation energy, and V_p and E_p are the electrostatic potential and the normal component of the electrostatic field generated on the surface by the transition density, respectively. η_S is the solvent refractive index measured in the visible spectrum far from electron transitions whereas $\Omega^S = \eta_S I$, with I being the first ionization potential of the solvent. To achieve a practical expression, a further simplification is introduced, by making use of an averaged excitation energy ω_{ave}, thereby eliminating the dependence of the prefactor of the surface integral on the excited state in eq 3. We also note that the parameter k_{disp}[12] was originally determined using Hartree−Fock calculations and the averaged excitation energy ω_{ave} was obtained by considering a predefined set of occupied and virtual orbitals defined by a window of energies and averaging for such a set. This choice is, however, strictly connected to the QM method employed.[28] To avoid that, a new parametrization has been more recently proposed[20] and the parameter k_{disp} is chosen to be solvent-dependent.

Each of the three interactions corresponds to a term in the effective Hamiltonian such that, electrostatic, dispersion, and repulsion effects will contribute to determine the solute wave function and the corresponding electron density. Moreover, the resulting effective Hamiltonian can also be generalized to calculate solvent effects on excitation energies using the common approaches developed for gas-phase molecules.

During the years, different strategies have been proposed to account for solvent effects on excitations using a PCM approach. The differences among the strategies arise not only from the type of interactions included (only electrostatic, electrostatic plus dispersion and repulsion) but also from the formulation used for the electrostatic contribution. These different formulations can be collected in two main families, the so-called linear response (LR)[29,30] and state-specific (SS)[31−33] approaches. By simplifying at most, we can say that in the LR formulation, the response of the solvent polarization to a given excitation "p" is computed from the transition density ρ_p (eq 4), whereas in the SS approach the same polarization is determined by the difference between ground and excited-state electron density ρ_{Δ_p} (eq 5):

$$\omega_{LR} = \omega_0 + \int_{\Gamma} V[\rho_p](s)\ \sigma[\varepsilon_\infty,\rho_p](s)\ ds \tag{4}$$

$$\omega_{SS} = \omega_0 + \frac{1}{2}\int_{\Gamma} V[\rho_{\Delta_p}](s)\ \sigma[\varepsilon_\infty,\rho_{\Delta_p}](s)\ ds \tag{5}$$

where in both cases a nonequilibrium response of the solvent has been used by introducing an optical dielectric constant ε_∞: this is justified if we describe the excitation as a vertical process and we assume that only the fast (or electronic) part of the solvent polarization will respond. In the two equations, ω_0 is the same quantity and it represents a "frozen solvent" contribution.

In the above equations nonelectrostatic effects are not explicitly accounted for. Because the repulsion operator derived from the interaction energy reported in eq 2 is a one-electron operator, repulsion does not give any explicit term in eq 4 and 5. However, the repulsion operator changes the ground-state orbitals, thus implicitly affecting ω through ω_0 and ρ_{Δ_p} or ρ_p. On the contrary, dispersion gives an explicit contribution (in addition to the implicit one): due to the nature of the expression here used (see eq 3), this contribution is independent of the LR or SS scheme (see below).

dx.doi.org/10.1021/jp507962n | J. Phys. Chem. B XXXX, XXX, XXX−XXX

If we now apply a TD-DFT framework, the LR transition energies and transition densities are obtained as eigenvalues and eigenvectors of the non-Hermitian eigensystem:

$$\begin{bmatrix} \mathbb{A} & \mathbb{B} \\ \mathbb{B}^* & \mathbb{A}^* \end{bmatrix} \begin{bmatrix} \mathbf{X} \\ \mathbf{Y} \end{bmatrix} = \omega_{\mathrm{LR}} \begin{bmatrix} \mathbf{1} & 0 \\ 0 & -\mathbf{1} \end{bmatrix} \begin{bmatrix} \mathbf{X} \\ \mathbf{Y} \end{bmatrix} \tag{6}$$

$\mathbb{A}$ and $\mathbb{B}$ being

$$\mathbb{A}_{ai,bj} = \delta_{ab}\delta_{ij}(\varepsilon_a - \varepsilon_i) + \langle ia|jb\rangle + f^{\mathrm{xc}}_{ai,bj} + V^{\mathrm{PCM}}_{ai,bj}$$
$$\mathbb{B}_{ai,bj} = \langle ia|bj\rangle + f^{\mathrm{xc}}_{ai,bj} + V^{\mathrm{PCM}}_{ai,bj} \tag{7}$$

where indices i, j, ... label occupied, and a, b, ... virtual molecular orbitals and ε_r are the corresponding orbital energies as obtained for the solvated ground-state solute. In eq 7 $f^{\mathrm{xc}}_{ai,bj}$ represents a matrix element of the exchange−correlation kernel in the adiabatic approximation whereas $V^{\mathrm{PCM}}_{ai,bj}$ is the corresponding matrix element of the PCM reaction potential which can be obtained as a second derivative with respect to the density of the electrostatic interaction energy reported in eq 1. In the same way we can also introduce dispersion effects starting from eq 3; as a result the PCM contribution is split into two terms, namely

$$\begin{aligned} V^{\mathrm{PCM}}_{ai,bj} &= V^{\mathrm{ele}}_{ai,bj} + V^{\mathrm{dis}}_{ai,bj} \\ &= \int_\Gamma \mathrm{d}s\, \sigma[\varepsilon_\infty, \psi_a^*\psi_i](s)\, V(\psi_b^*\psi_j)(s) \\ &\quad + \beta \int_\Gamma \mathrm{d}s\, V(\psi_a^*\psi_i)(s)\, E(\psi_b^*\psi_j)(s) \end{aligned} \tag{8}$$

In eq 8 we have introduced the factor β which, following what reported in eq 3, is defined as

$$\beta = k_{\mathrm{dis}} \frac{\eta_S^{\,2} - 1}{\eta_S^{\,2}} \frac{\Omega^S}{\Omega^S + \omega_{\mathrm{ave}}} \tag{9}$$

This factor is, however, optimized for a ground-state system. To extend the same approach to excited states we should recalculate it for each state. Here, however, we have preferred to keep the formulation as simple as possible and to introduce a single scaling parameter c_s for all the excitations that we have determined through a fitting procedure (see below).

We note that the ω_0 term in eqs 4 and 5 can be recovered by neglecting $V^{\mathrm{PCM}}_{ai,bj}$ in the resolution of the matrix equation (eq 6). On the contrary, if we want to determine ω_{SS} we have to go a step farther and calculate the relaxation of the ground-state electron density due to the excitation. This relaxation contribution can be obtained within the LR-TDDFT scheme in terms of the so-called **Z**-vector approach,[34,35] which has been generalized to the PCM-electrostatic approach by Scalmani et al.[36] By knowing the resulting electron density, we obtain the second term in the right-hand side of eq 5 by simply calculating the fast component of the PCM surface charge, $\sigma[\varepsilon_\infty, \rho_{\Delta_p}]$. As a matter of fact, an iterative approach should be introduced to obtain mutually equilibrated values of σ and ρ_{Δ_p}.[33] However, if we assume that ρ_{Δ_p} is small and we note that the correction term in eq 5 is quadratic in ρ_{Δ_p}, we can just stop at the first-order level of the iteration and obtain what is known as *corrected linear response* (cLR) scheme,[31] which can be seen as a first-order approximation to the state-specific excitation energy. In the present work, the cLR approach is particularly justified, as the electrostatic term in eq 5 should be small enough.

3. COMPUTATIONAL DETAILS

We performed excited-state calculations on a set of chromophores presenting different kinds of transitions. Such a set includes n → π^* chromophores (acetone, acrolein, pyridine, pyrazine, pyrimidine, and pyridazine) and $\pi \rightarrow \pi^*$ aromatic chromophores (benzene, naphthalene, anthracene). Geometries were optimized *in vacuo* at the B3LYP/6-311G(d) level of theory and assumed unchanged upon solvation. For all the calculations, cyclohexane was used as solvent.

The dependence on the density functional was assessed by comparing various functionals, with different weights of exact exchange, and Hartree−Fock. All calculations were run using the 6-311+G(2d,2p) split valence basis set.

To evaluate the extent of the coupling between the electrostatic and nonelectrostatic interactions, we adopted five different schemes, in which different solute−solvent interactions are included in the PCM effective Hamiltonian. The labels PCM(EDR) refer to the interactions included in the Hamiltonian, where E means *electrostatic*, D means *dispersion*, and R means *repulsion*. We employed the M06-2X/6-311+G(2d,2p) level of theory for this and all the following calculations. For the inclusion of electrostatic interactions we employed the two different methods described in the Methods, namely LR and cLR.

Finally, we parametrized the dispersion contribution to the TDDFT matrices by minimizing the root-mean-square (RMS) error between the calculated and the experimental solvatochromic shift within the set of selected excitations.

All the calculations were run applying the Tamm−Dancoff approximation (TDA)[37] of the TDDFT formulation and using a locally modified version of the Gaussian09 suite of codes.[38] The electrostatic contribution was obtained using the IEF version[26] of PCM together with a cavity and surface discretization procedure into point charges available in Gaussian09 asking for the Gaussian03 defaults. The molecular cavities were built using Bondi radii scaled by 1.2.

4. RESULTS AND DISCUSSION

4.1. Dependence on the DFT Functional. As a preliminary analysis we have investigated the dependence of the PCM(EDR) approach on the DFT functional used. In particular, the attention has been focused on the role of the percentage of exact exchange included in the functional. To this aim we have selected five functionals, with different weights of exact exchange, LDA,[39,40] PBE,[41,42] B3LYP,[43] M06-2X,[44] ωB97X,[45] and HF, together with the 6-311+G(2d,2p) split valence basis set.

As the electrostatic contribution is known to be weakly dependent on the specific functional used, here the analysis has been limited to the dispersion-only description. Moreover, to have a more direct analysis, we have focused on "frozen solvent" excitation energies ω_0, obtained by including the dispersion contribution only in the ground-state calculation, but not in the response matrices (eq 7).

Figure 1 shows the dependence of ω_0 excitation energies on the percentage of exact exchange in the functional used. We considered the shifts with respect to gas phase, normalized to the shift predicted by the HF method, as in eq 10.

dx.doi.org/10.1021/jp507962n | J. Phys. Chem. B XXXX, XXX, XXX−XXX

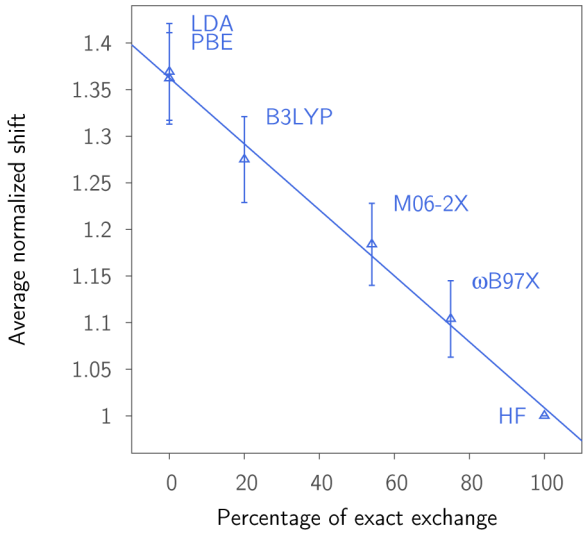

Figure 1. Dependence of the average normalized dispersion shift on the percentage of exact exchange in the functional used. Because ωB97X is a *range-separated* hybrid, with the HF exchange ranging from 16% to 100%, we used an "average" value of 75% for the percentage of HF exchange. The error bars represent a standard deviation. The regression line has a slope of 3.54×10^{-3}, an intercept of 1.36, and $R^2 = 0.9945$.

$$\Delta\omega_0^{(\mathrm{Norm})} = \frac{\omega_0^{(\mathrm{Func})} - \omega_{\mathrm{vac}}^{(\mathrm{Func})}}{\omega_0^{(\mathrm{HF})} - \omega_{\mathrm{vac}}^{(\mathrm{HF})}} \tag{10}$$

The normalized values were averaged over the first transitions of each chromophore, thus eliminating the dependence on the type of transition. The variation of ω_0 excitation energy reflects the variation of the occupied and virtual orbitals in the ground state and provides information on the Fock dispersion operator. The behavior of ω_0 values is almost linear with the fraction of exact exchange ($R^2 = 0.9945$), and we see a 35% variation of ω_0 between the two extremes (HF and pure DFs). However, the most commonly used functionals fall in the same range, and the difference between B3LYP and M06-2X is only about 8%.

From the results obtained so far, we can guess that the dispersion contribution to the PCM matrix elements, $V_{ai,bj}^{\mathrm{PCM}}$, and thus its effect on the transition properties, becomes stronger in those functionals that have a small percentage of exact exchange, supposedly because the predicted occupied-virtual orbital energy gap lowers with such functionals, and the dispersion operator implicitly depends on this gap.[28]

For all the following analyses we have selected the M06-2X[44] functional, which presents almost 54% of exact exchange: this functional has in fact been shown to give very good results for the prediction of electronic excitation energies of main-group compounds by time-dependent density functional theory.[46−48]

4.2. Couplings among Electrostatic and Nonelectrostatic Contributions. For each molecule of the set, we report in Figure 2 the dispersion−repulsion coupling (Δ_{DR}), which is defined as the difference between the gas to cyclohexane solvatochromic shift calculated with the PCM(DR) scheme and the sum of those calculated with the PCM(R) and the PCM(D) schemes. Similarly, the dispersion−repulsion−electrostatic (Δ_{EDR}) coupling is defined as the difference between the PCM(EDR) results and the sum of the PCM(DR) and the PCM(E) contributions.

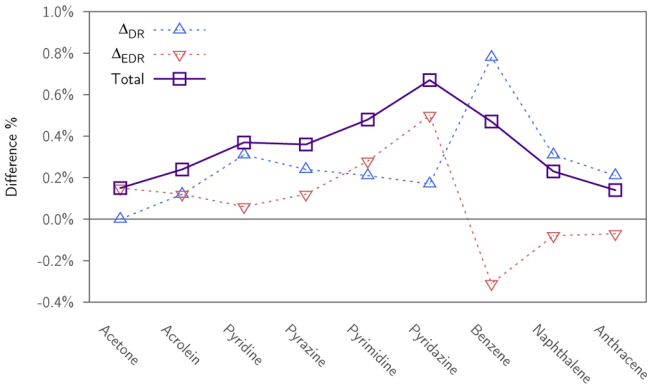

Figure 2. Plot of Δ_{DR} and Δ_{EDR} as error on the total shift, along with the *total* difference between the PCM(EDR) calculation and the sum of electrostatic, dispersion and repulsion contributions. These values are always less than 1% and therefore negligible. Δ_{DR} is defined as $[(\Delta\omega_{\mathrm{DR}} - \Delta\omega_{\mathrm{D}} - \Delta\omega_{\mathrm{R}})/\Delta\omega_{\mathrm{DR}}] \times 100\%$, and Δ_{EDR} is defined as $[(\Delta\omega_{\mathrm{EDR}} - \Delta\omega_{\mathrm{E}} - \Delta\omega_{\mathrm{D}} - \Delta\omega_{\mathrm{R}})/\Delta\omega_{\mathrm{EDR}}] \times 100\%$.

Both Δ_{DR} and Δ_{EDR} couplings are found to be zero or negligible for any transition we considered. We conclude that the repulsion, dispersion, and electrostatic contributions to the excitation energy are almost additive; this allows us to tackle one contribution at a time and focus the parametrization on the dispersion part only, neglecting its influence on the other contributions. Moreover, we can rely on the quasi additivity of the nonelectrostatic and electrostatic shifts to use the *corrected linear response* scheme for the ES contribution, which will be calculated separately. This result supports the use of models where the solvatochromic shift is calculated as a sum of different (electrostatic and nonelectrostatic) contributions, as in the scheme recently proposed by Marenich et al.[21,22] The coupling between electrostatic and nonelectrostatic contribution was found to be larger but still rather limited (2−4%) also for ground-state solvation energies.[28]

4.3. Dispersion Contribution. As commented in the Methods, the factor β appearing in the dispersion expression was originally obtained for ground-state solutes (k_{dis} was optimized with respect to solvation free energies).[20] To adapt the same expression to excitation processes, we adopt here a double-step strategy: we use the previously optimized β factor for ground-state calculations and we rescale it with a suitable parameter c_s when used to calculate the components, $V_{ai,bj}^{\mathrm{dis}}$, of the PCM response matrix.

Figure 3 shows, as an example, the solvatochromic shift of the L_a and L_b transitions of anthracene at different values of the LR operator scaling c_s.

In this case, along with all the other transitions tested, we can see that the behavior of the excitation energy is perfectly linear in c_s, so that we can choose a reasonable value for c_s, which will reduce the errors in the solvatochromic shifts. To obtain the optimal c_s coefficient for each transition, we considered experimental vacuum-to-solvent excitation energy shifts as a reference and found, through the linear calibration curve, the value of c_s that gives the best agreement.

Although the electrostatic effects are not dominant in nonpolar solvent, we have to include them in our calculations to make sure that our fitted parameter accounts only for the dispersion contribution to the excitation energy shift. As reported in the Methods, there are alternative approaches for the inclusion of electrostatic effects in an excitation process.

dx.doi.org/10.1021/jp507962n | J. Phys. Chem. B XXXX, XXX, XXX−XXX

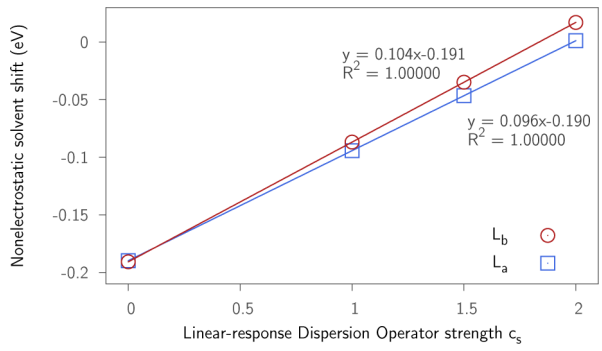

Figure 3. Solvatochromic shift (nonelectrostatic component only) of L_a and L_b transitions of anthracene. The linear fit is also shown for both transitions.

Here, we focus on the LR and cLR models. Finally, the contribution from repulsion was included in all the calculations.

We took as references the experimental gas to cyclohexane spectral shifts, where they were available, or to another similar solvent. The chromophores used in the parametrization are listed in Table 1 along with the experimental shifts; the calculated *gas-phase* transition energies and experimental absorption maxima are reported in the Supporting Information (Table S5). It should be noted that this comparative procedure presents an intrinsic uncertainty, because the calculated quantity, a shift in the *vertical excitation energy*, is not directly available experimentally. The shift in the band maximum is commonly used to approximate the variation in vertical excitation energies, but the uncertainty in the comparison should be kept in mind, especially because we want to use this comparison to fit an empirical parameter to use in our model. For this reason, we also estimated an error in the value of c_s assuming that there is an uncertainty of 50 cm^{-1} in the experimentally derived shifts.

Table 1. Chromophores and Transitions Employed for the Parametrization, along with the Experimental Vacuum to Solvent Shifts (cm^{-1})[a]

chromophore	transition	$\Delta\omega$ (exptl)	notes
acetone	$n\pi^*$	−55	in *n*-decane[49]
pyridine	$\pi\pi^*$	−325	in isooctane[50]
pyrazine	$n\pi^*$	−400	in cyclohexane[51]
	$\pi\pi^*$	−550	
pyrimidine	$n\pi^*$	−200	in cyclohexane[52]
	$\pi\pi^*$	−320	in methylcyclohexane[53]
pyridazine	$\pi\pi^*$	−130	in cyclohexane[51] and *in vacuo*[54]
benzene	L_b	−308	from ref 55
	L_a	−1070	
naphthalene	L_b	−296	from ref 56
	L_a	−954	
anthracene	L_a	−1030	from ref 57
	B_b	−2917	

[a]When the shifts were not available, we took the solvent shift as the difference in the most intense vibronic peak in the gas-phase and solvent spectra. If not reported differently, gas-phase data are from ref 58.

We choose the parameter c_s by minimizing the RMS error E between the calculated and the experimental shift within the set presented in Table 1:

$$E = \sqrt{\frac{\sum_k (\Delta\omega_k^{calc} - \Delta\omega_k^{exp})^2}{N}}$$

$\Delta\omega_k^{calc}$ is a function of the only parameter c_s. Because the behavior of $\Delta\omega$ for all the transitions is perfectly linear with c_s, we can write $\Delta\omega_k^{calc} = a_k + b_k \cdot c_s$, and find analytically the optimal value for c_s.

We report in Table 2 the optimal c_s values, calculated using two different schemes for electrostatic, LR and cLR, along with the RMS and maximum absolute error.

Table 2. Results for the Fitting of the c_s Parameter, Employing Two Different Schemes for the Electrostatic Contribution[a]

model	optimal c_s	RMS error	MAE
LR	1.510 ± 0.005	295	759
cLR	1.232 ± 0.005	368	837

[a]RMS and MAE values are in cm^{-1}.

We see that the both schemes yield $c_s > 1$, even if with fairly different values, and with the LR scheme giving slightly smaller errors. A fitted $c_s > 1$ s not unexpected. In fact, for a solvated molecule in an excited state, the dispersion energy receives a contribution also from de-excitations. By adopting a simplified scheme, we can write from eq 3

$$\frac{c_s}{\Omega^S + \omega_{ave}} \approx \frac{p_I}{\Omega^S + \omega_{ave}^I} + \frac{p_{II}}{\Omega^S - \omega_{ave}^{II}} \quad (11)$$

in which we distinguish explicitly two contributions to the average, one from excitations to higher energy states (I) and one from de-excitations to lower energy states (II). By putting $\omega_{ave}^I + \omega_{ave}^{II} = \omega_{ave}$ and assuming for the weight a simple expression like $p_I = \omega_{ave}^I/\omega_{ave}$, we have almost immediately

$$c_s \approx \frac{p_I(\Omega^S + \omega_{ave})}{\Omega^S + p_I\omega_{ave}} + \frac{(1-p_I)(\Omega^S + \omega_{ave})}{\Omega^S - (1-p_I)\omega_{ave}} \quad (12)$$

This equation leads to $c_s = 1$ when $p_I = 1$ and $c_s > 1$ when $p_I < 1$ in agreement with our finding. This simple analysis also tells us also that c_s should depend on the solvent through Ω^S.

To assess if our model is capable of reproducing the trend in solvent shifts, we report, for both LR and cLR schemes, the correlation plots between experimental and calculated shifts (Figure 4).

From the analysis of these plots we can make some considerations. First, the LR electrostatic scheme better differentiates between the various transitions, whereas the cLR scheme yields shifts that are too similar, resulting in a smaller correlation between calculated and experimental values. Second, we can recognize two sets of transitions, denoted with different marks in the plot; one includes nonpolar chromophores (benzene, naphthalene, and anthracene, only $\pi \rightarrow \pi^*$ transitions), whose shifts are typically underestimated by our model, whereas the other includes polar chromophores (acetone, pyridine, and the diazines, with both $\pi \rightarrow \pi^*$ and n $\rightarrow \pi^*$ transitions), whose shifts are overestimated. We also note that there is one particular transition, the L_a transition of benzene, that appears to be an outlier, as it lies too far from the nonpolar trendline and corresponds to the maximum error between calculated and experimental shift in both electrostatic schemes: this transition is the responsible of the MAE values of

dx.doi.org/10.1021/jp507962n | J. Phys. Chem. B XXXX, XXX, XXX−XXX

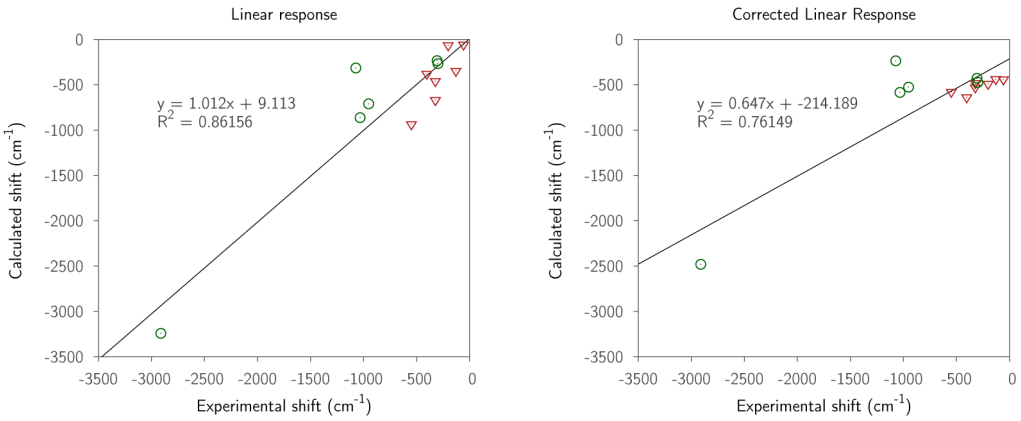

Figure 4. Correlation of experimental and calculated solvent spectral shifts (cm^{-1}). The plot on the left was obtained using the *linear response* (LR) scheme for the electrostatic contribution, and the plot on the right was obtained using the *corrected linear response* (cLR) scheme. Circles represent nonpolar aromatic hydrocarbons (benzene, naphthalene, anthracene), and triangles represent polar chromophores (acetone, pyridine, and diazines).

759 cm^{-1} (LR) and 857 cm^{-1} (cLR) reported in Table 2. The unexpectedly low red shift predicted by our model for benzene L_a can be partially explained in terms of an overestimation of the repulsion component, which corresponds to a blue shift of 320 cm^{-1} (Supporting Information). This may be due to a mixing of $\pi \rightarrow \pi^*$ and Rydberg states in the TD-DFT description of this transition.

4.4. Discussion. To investigate deeper the results obtained above, we summarize here the analysis done by Corni et al.[59] based on a simple model for the solute−solvent system that bypasses one of the basic assumptions of continuum solvation models, i.e., the use of a single Hartree product of a solute and a solvent wave function to describe the total solute−solvent wave function. In such an analysis the total wave function was described as a linear combination of the four products of two solute states and two solvent electronic states. The solute excitation energy resulting from such an analysis is here rewritten in a form reminiscent of the Onsager model for solute−solvent interactions (a dipolar solute in a spherical cavity):

$$\omega = \omega_0 - \frac{1}{2} g_e (\mu_{GS} - \mu_{ES})^2 - g_e^d |\mu^T|^2 - \frac{1}{2\pi} \int_0^\infty d\omega\, g(i\omega)\, \Delta\alpha(i\omega)$$
$$= \omega_0 - \omega_{Ele} - \omega_{Res} - \omega_D \qquad (13)$$

where g_e is the linear electronic response of the solvent (and it can be interpreted as the Onsager-like nonequilibrium response function of the solvent), μ_{GS} and μ_{ES} are the ground and excited-state electric dipoles of the solute, and μ^T is the transition dipole between them.

As already commented, the first term on the right-hand side of eq 13, ω_0, takes into account the polarization of the solvent with respect to the ground-state electron density; the second term contains the square of the difference between the response of the solvent electronic polarization to the ground-state and excited-state densities and is a purely electrostatic term. The third term depends on the transition density between the ground and excited state (that is, in a dipolar approximation, to the square of the transition dipole); this contribution, which we shall call the "resonance" term, is identifiable with the Bayliss equation for the spectral shift in nonpolar solvents[17] and is sometimes considered a dispersion effect.[18,59,60] The last term is the "pure" dispersion term, namely, the difference in dispersion energies of ground and excited states. We also note that the last three terms depend on the same solvent parameter ε_∞. In polar solvents, ω_0 is the dominant one, because it is the only term that is determined by the full response of the solvent (including also the orientational polarization). However, in nonpolar solvents, all four terms can be of the same magnitude.

When eq 13 is compared with the LR and cLR equations (eqs 4 and 5), it is evident that the LR and the cLR schemes contain different subsets of the total number of terms. In particular, the cLR model, as expected from its purely electrostatic nature, includes only the first and the second term (or better a first-order approximation of that), whereas the LR, unexpectedly, includes the first and the third term even if the latter is not a real electrostatic term. In the original analysis, the LR "ambiguity" was related to the incapability of the effective Hamiltonian of QM/continuum models to correctly describe energy expectation values of not stationary solute states. Because in a perturbation approach, such as the LR treatment, the perturbed state can be seen as a linear combination of zeroth-order states, a wrong partition of the solvent terms among the various perturbation orders is obtained. In the same analysis, the LR contribution was described as part of the dispersion term together with the "pure" one.

The present analysis seems to confirm this physical interpretation for the following reasons. When a nonpolar solvent is considered, the electrostatic contribution is expected to be rather small if not negligible (especially if the transition does not lead to significant electron density variations). As a result, the cLR contribution when combined with the "pure" dispersion term should not change the correlations between calculated and experimental gas-to-nonpolar shifts. On the contrary, the combination of "resonance" and "pure" dispersion contributions (i.e., the coupling of dispersion and LR results) should give a better estimation of the real solvent effects as they both account for nonelectrostatic effects. This is indeed what we have observed in the graphs reported in Figure 4. We note that models that introduce semiempirical corrections of the excitation energies naturally include the "resonance" and "pure" dispersion contributions.[21,61,62]

5. SUMMARY

In this paper we have investigated the limits and potentialities of PCM in describing the gas-to-nonpolar solvent shift of

dx.doi.org/10.1021/jp507962n | J. Phys. Chem. B XXXX, XXX, XXX−XXX

excitation energies for solvated systems. The analysis has been performed by combining electrostatic and nonelectrostatic terms in the solute effective Hamiltonian and in the resulting TD-DFT equations (here applied in their TDA version). The results obtained using a reparameterized version of the Amovilli and Mennucci dispersion formulation[12] seem to show that in nonpolar solvents the role of electrostatic effects is almost null, as expected, but that instead the inclusion of the so-called "resonance" contribution can significantly improve the correlation with experiments. This term in the literature has been already included in the dispersion contribution[17,18,59,60] but in most of the continuum model calculations represents the electrostatic response to the solute electronic transition. Our analysis seems to confirm the first interpretation and it suggests that the so-called LR formulation of continuum models for electronic excitations should be taken with care as it introduces a nonelectrostatic response which, if treated alone, could lead to unbalanced effects. On the contrary, the cLR, or other SS approaches, are much safer approaches to include electrostatic responses and they can be always combined with dispersion (and repulsion) models possibly including also the "resonance" term.[22]

■ ASSOCIATED CONTENT

Supporting Information

Dispersion-induced excitation energy shifts used to obtain Figure 1; excitation energy shifts calculated with different PCM schemes used to obtain Figure 3; DR component of the excitation energy shifts (eV), at different values of the fitting parameter c_s; electrostatic and nonelectrostatic components of the excitation energy shifts; calculated gas-phase vertical transition energies. This material is available free of charge via the Internet at http://pubs.acs.org.

■ AUTHOR INFORMATION

Corresponding Authors

*L. Cupellini. E-mail: lorenzo.cupellini@for.unipi.it.
*C. Amovilli. E-mail: claudio.amovilli@unipi.it.
*B. Mennucci. E-mail: benedetta.mennucci@unipi.it.

Notes

The authors declare no competing financial interest.

■ ACKNOWLEDGMENTS

L.C. and B.M. acknowledge the European Research Council (ERC) for financial support in the framework of the Starting Grant (EnLight-277755).

■ REFERENCES

(1) Warshel, A.; Levitt, M. Theoretical Studies of Enzymic Reactions: Dielectric, Electrostatic and Steric Stabilization of The Carbonium Ion in The Reaction of Lysozyme. *J. Mol. Biol.* **1976**, *103*, 227−249.

(2) Field, M. J.; Bash, P. A.; Karplus, M. A Combined Quantum Mechanical and Molecular Mechanical Potential for Molecular Dynamics Simulations. *J. Comput. Chem.* **1990**, *11*, 700−733.

(3) Gao, J. Hybrid Quantum and Molecular Mechanical Simulations: An Alternative Avenue to Solvent Effects in Organic Chemistry. *Acc. Chem. Res.* **1996**, *29*, 298−305.

(4) Lin, H.; Truhlar, D. G. QM/MM: What Have We Learned, Where Are We, and Where Do We Go from Here? *Theor. Chem. Acc.* **2007**, *117*, 185−199.

(5) Senn, H. M.; Thiel, W. QM/MM Methods for Biomolecular Systems. *Angew. Chem., Int. Ed.* **2009**, *48*, 1198−1229.

(6) Olsen, J. M. H.; Kongsted, J. In *Molecular Properties through Polarizable Embedding*; Sabin, J. R., Brändas, E., Eds.; Advances in Quantum Chemistry; Academic Press: New York, 2011; Vol. *61*, Chapter 3, pp 107 − 143.

(7) Rivail, J. L.; Rinaldi, D. A Quantum Chemical Approach to Dielectric Solvent Effects in Molecular Liquids. *Chem. Phys.* **1976**, *18*, 233−242.

(8) Tomasi, J.; Persico, M. Molecular-Interactions in Solution - an Overview of Methods Based on Continuous Distributions of the Solvent. *Chem. Rev.* **1994**, *94*, 2027−2094.

(9) Cramer, C.; Truhlar, D. Implicit Solvation Models: Equilibria, Structure, Spectra, and Dynamics. *Chem. Rev.* **1999**, *99*, 2161−2200.

(10) Orozco, M.; Luque, F. J. Theoretical Methods for the Description of the Solvent Effect in Biomolecular Systems. *Chem. Rev.* **2000**, *100*, 4187−4226.

(11) Tomasi, J.; Mennucci, B.; Cammi, R. Quantum Mechanical Continuum Solvation Models. *Chem. Rev.* **2005**, *105*, 2999−3093.

(12) Amovilli, C.; Mennucci, B. Self-Consistent-Field Calculation of Pauli Repulsion and Dispersion Contributions to the Solvation Free Energy in the Polarizable Continuum Model. *J. Phys. Chem. B* **1997**, *101*, 1051−1057.

(13) Pomogaeva, A.; Chipman, D. M. New Implicit Solvation Models for Dispersion and Exchange Energies. *J. Phys. Chem. A* **2013**, *117*, 5812−20.

(14) Pomogaeva, A.; Chipman, D. M. Hydration Energy from a Composite Method for Implicit Representation of Solvent. *J. Chem. Theory Comput.* **2014**, *10*, 211−219.

(15) Mennucci, B. Polarizable Continuum Model. *Wiley Interdiscip. Rev. Comput. Mol. Sci.* **2012**, *2*, 386−404.

(16) Barone, V.; Baiardi, A.; Biczysko, M.; Bloino, J.; Cappelli, C.; Lipparini, F. Implementation And Validation of a Multi-Purpose Virtual Spectrometer for Large Systems in Complex Environments. *Phys. Chem. Chem. Phys.* **2012**, *14*, 12404−12422.

(17) Bayliss, N. The Effect of The Electrostatic Polarization of the Solvent on Electronic Absorption Spectra in Solution. *J. Chem. Phys.* **1950**, *18*, 292−296.

(18) Roesch, N.; Zerner, M. Calculation of Dispersion Energy Shifts in Molecular Electronic Spectra. *J. Phys. Chem.* **1994**, 5817−5823.

(19) Renger, T.; Grundkötter, B.; Madjet, M. E.-A.; Müh, F. Theory of Solvatochromic Shifts in Nonpolar Solvents Reveals a New Spectroscopic Rule. *Proc. Natl. Acad. Sci. U. S. A.* **2008**, *105*, 13235−13240.

(20) Weijo, V.; Mennucci, B.; Frediani, L. Toward a General Formulation of Dispersion Effects for Solvation Continuum Models. *J. Chem. Theory Comput.* **2010**, *6*, 3358−3364.

(21) Marenich, A. V.; Cramer, C. J.; Truhlar, D. G. Uniform Treatment of Solute-Solvent Dispersion in the Ground and Excited Electronic States of the Solute Based on a Solvation Model with State-Specific Polarizability. *J. Chem. Theory Comput.* **2013**, 3649−3659.

(22) Marenich, A. V.; Cramer, C. J.; Truhlar, D. G. Electronic Absorption Spectra and Solvatochromic Shifts by the Vertical Excitation Model: Solvated Clusters and Molecular Dynamics Sampling. *J. Phys. Chem. B* **2014**, DOI: 10.1021/jp506293w.

(23) Miertus, S.; Scrocco, E.; Tomasi, J. Electrostatic Interaction of a Solute With a Continuum. A Direct Utilization of Ab-Initio Molecular Potentials for the Prevision of Solvent Effects. *Chem. Phys.* **1981**, *55*, 117−129.

(24) Cammi, R.; Tomasi, J. Remarks on the Use of the Apparent Surface Charges (ASC) Methods in Solvation Problems: Iterative versus Matrix-Inversion Procedures and the Renormalization of the Apparent Charges. *J. Comput. Chem.* **1995**, *16*, 1449−1458.

(25) Barone, V.; Cossi, M. Quantum Calculation of Molecular Energies and Energy Gradients in Solution by a Conductor Solvent Model. *J. Phys. Chem. A* **1998**, *102*, 1995−2001.

(26) Cances, E.; Mennucci, B.; Tomasi, J. A New Integral Equation Formalism for the Polarizable Continuum Model: Theoretical Background and Applications to Isotropic and Anisotropic Dielectrics. *J. Chem. Phys.* **1997**, *107*, 3032−3041.

(27) Amovilli, C. Calculation of The Dispersion Energy Contribution to the Solvation Free Energy. *Chem. Phys. Lett.* **1994**, *229*, 244−249.

(28) Curutchet, C.; Orozco, M.; Luque, F. J.; Mennucci, B.; Tomasi, J. Dispersion and Repulsion Contributions to the Solvation Free Energy: Comparison of Quantum Mechanical and Classical Approaches in the Polarizable Continuum Model. *J. Comput. Chem.* **2006**, *27*, 1769−1780.
(29) Cammi, R.; Mennucci, B. Linear Response Theory for the Polarizable Continuum Model. *J. Chem. Phys.* **1999**, *110*, 9877−9886.
(30) Cossi, M.; Barone, V. Time-Dependent Density Functional Theory for Molecules in Liquid Solutions. *J. Chem. Phys.* **2001**, *115*, 4708−4717.
(31) Caricato, M.; Mennucci, B.; Tomasi, J.; Ingrosso, F.; Cammi, R.; Corni, S.; Scalmani, G. Formation and Relaxation of Excited States in Solution: A New Time Dependent Polarizable Continuum Model Based on Time Dependent Density Functional Theory. *J. Chem. Phys.* **2006**, *124*, 124520−124513.
(32) Improta, R.; Barone, V.; Scalmani, G.; Frisch, M. J. A State-Specific Polarizable Continuum Model Time Dependent Density Functional Theory Method for Excited State Calculations in Solution. *J. Chem. Phys.* **2006**, *125*, 054103.
(33) Marenich, A. V.; Cramer, C. J.; Truhlar, D. G.; Guido, C. A.; Mennucci, B.; Scalmani, G.; Frisch, M. J. Practical Computation of Electronic Excitation in Solution: Vertical Excitation Model. *Chem. Sci.* **2011**, *2*, 2143−2161.
(34) Handy, N. C.; Schaefer, H. F. On the Evaluation of Analytical Energy Derivatives for Correlated Wave Functions. *J. Chem. Phys.* **1984**, *81*, 5031−5033.
(35) Foresman, J.; Head-Gordon, M.; Pople, J.; Frisch, M. Toward A Systematic Molecular-Orbital Theory For Excited-States. *J. Phys. Chem-Us* **1992**, *96*, 135−149.
(36) Scalmani, G.; Frisch, M.; Mennucci, B.; Tomasi, J.; Cammi, R.; Barone, V. Geometries and Properties of Excited States in the Gasand in Solution: Theory and Application of a Time-Dependent Density Functional Theory Polarizable Continuum Model. *J. Chem. Phys.* **2006**, *124*, 094107−094115.
(37) Hirata, S.; Head-Gordon, M. Time-Dependent Density Functional Theory within the Tamm−Dancoff Approximation. *Chem. Phys. Lett.* **1999**, *314*, 291−299.
(38) Frisch, M. J.; Trucks, G. W.; Schlegel, H. B.; Scuseria, G. E.; Robb, M. A.; Cheeseman, J. R.; Scalmani, G.; Barone, V.; Mennucci, B.; Petersson, G. A.; Nakatsuji, H.; Caricato, M.; Li, X.; Hratchian, H. P.; Izmaylov, A. F.; et al. *Gaussian 09*, Revision D.01; Gaussian Inc.: Wallingford, CT, 2009.
(39) Slater, J. Comparison of TFD and X*a* Methods for Molecules and Solids. *Int. J. Quantum Chem. Symp.* **195**, *9*, 7−21.
(40) Vosko, S. H.; Wilk, L.; Nusair, M. Accurate Spin-Dependent Electron Liquid Correlation Energies for Local Spin Density Calculations: A Critical Analysis. *Can. J. Phys.* **1980**, *58*, 1200−1211.
(41) Perdew, J. P.; Burke, K.; Ernzerhof, M. Generalized Gradient Approximation Made Simple. *Phys. Rev. Lett.* **1996**, *77*, 3865−3868.
(42) Perdew, J. P.; Burke, K.; Ernzerhof, M. Generalized Gradient Approximation Made Simple [Phys. Rev. Lett. 77, 3865 (1996)]. *Phys. Rev. Lett.* **1997**, *78*, 1396−1396.
(43) Becke, A. D. Density-Functional Thermochemistry. III. The Role of Exact Exchange. *J. Chem. Phys.* **1993**, *98*, 5648−5652.
(44) Zhao, Y.; Truhlar, D. G. The M06 Suite of Density Functionals for Main Group Thermochemistry, Thermochemical Kinetics, Noncovalent Interactions, Excited States, and Transition Elements: Two New Functionals and Systematic Testing of Four M06-Class Functionals and 12 Other Functionals. *Theor. Chem. Acc.* **2008**, *120*, 215−241.
(45) Chai, J.-D.; Head-Gordon, M. Systematic Optimization of Long-Range Corrected Hybrid Density Functionals. *J. Chem. Phys.* **2008**, *128*, 084106.
(46) Jacquemin, D.; Perpète, E. A.; Ciofini, I.; Adamo, C.; Valero, R.; Zhao, Y.; Truhlar, D. G. On the Performances of the M06 Family of Density Functionals for Electronic Excitation Energies. *J. Chem. Theory Comput* **2010**, *6*, 2071−2085.
(47) Li, R.; Zheng, J.; Truhlar, D. G. Density Functional Approximations for Charge Transfer Excitations with Intermediate Spatial Overlap. *Phys. Chem. Chem. Phys.* **2010**, *12*, 12697.
(48) Leang, S. S.; Zahariev, F.; Gordon, M. S. Benchmarking the Performance of Time-Dependent Density Functional Methods. *J. Chem. Phys.* **2012**, *136*, 104101.
(49) Renge, I. Solvent Dependence of n-π^* Absorption in Acetone. *J. Phys. Chem. A* **2009**, *113*, 10678−10686.
(50) Stephenson, H. P. Solution Spectra and Oscillator Strengths of Electronic Transitions of Pyridine and Some Monosubstituted Derivatives. *J. Chem. Phys.* **1954**, *22*, 1077−1082.
(51) Halverson, F.; Hirt, R. C. Near Ultraviolet Solution Spectra of the Diazines. *J. Chem. Phys.* **1951**, *19*, 711−718.
(52) Baba, H.; Goodman, L.; Valenti, P. C. Solvent Effects on the Fluorescence Spectra of Diazines. Dipole Moments in the (n, p^*) Excited States 1. *J. Am. Chem. Soc.* **1966**, *88*, 5410−5415.
(53) Clark, L. B.; Tinoco, I. Correlations in the Ultraviolet Spectra of the Purine and Pyrimidine Bases. *J. Am. Chem. Soc.* **1965**, *87*, 11−15.
(54) Holland, D. M. P.; Shaw, D.; Coriani, S.; Stener, M.; Decleva, P. A Study of the Valence Shell Electronic States of Pyridazine by Photoabsorption Spectroscopy and Time-Dependent Density Functional Theory Calculations. *J. Phys. B: Atomic, Molecular and Optical Physics* **2013**, *46*, 175103.
(55) Bayliss, N.; Hulme, L. Solvent Effects in the Spectra of Benzene, Toluene and Chlorobenzene at 2600 and 2000 Å. *Aust. J. Chem.* **1953**, *6*, 257−277.
(56) Weigang, O. E. Spectral Solvent Shift. I. Paraffin Hydrocarbon Solvent Interactions with Polynuclear Aromatic Hydrocarbons. *J. Chem. Phys.* **1960**, *33*, 892−899.
(57) Morales, R. G. E. Polarizability Change in the Excited Electronic States of Nonpolar Aromatic Hydrocarbons. *J. Phys. Chem.* **1982**, *86*, 2550−2552.
(58) Bolovinos, A.; Tsekeris, P.; Philis, J.; Pantos, E.; Andritsopoulos, G. Absolute Vacuum Ultraviolet Absorption Spectra of Some Gaseous Azabenzenes. *J. Mol. Spectrosc.* **1984**, *103*, 240−256.
(59) Corni, S.; Cammi, R.; Mennucci, B.; Tomasi, J. Electronic Excitation Energies of Molecules in Solution within Continuum Solvation Models: Investigating the Discrepancy between State-Specific and Linear-Response Methods. *J. Chem. Phys.* **2005**, *123*, 134512.
(60) Zhu, C.; Dalgarno, A.; Porsev, S.; Derevianko, A. Dipole Polarizabilities of Excited Alkali-Metal Atoms and Long-Range Interactions of Ground- and Excited-State Alkali-Metal Atoms with Helium Atoms. *Phys. Rev. A* **2004**, *70*, 032722.
(61) Li, J.; Cramer, C. J.; Truhlar, D. G. Two-Response-Time Model Based On CM2/INDO/S2 Electrostatic Potentials for the Dielectric Polarization Component of Solvatochromic Shifts on Vertical Excitation Energies. *Int. J. Quantum Chem.* **2000**, *77*, 264−280.
(62) Marenich, A. V.; Cramer, C. J.; Truhlar, D. G. Sorting Out the Relative Contributions of Electrostatic Polarization, Dispersion, and Hydrogen Bonding to Solvatochromic Shifts on Vertical Electronic Excitation Energies. *J. Chem. Theory Comput.* **2010**, *6*, 2829−2844.